THE JOURNAL OF PHYSICAL CHEMISTRY A LETTERS

2008, *112,* 166−171
Published on Web 12/22/2007

Microwave Catalysis through Rotationally Hot Reactive Species†

Urban Bren, Andrej Kržan, and Janez Mavri*

National Institute of Chemistry, Hajdrihova 19, SI-1001 Ljubljana, Slovenia

Received: October 5, 2007; In Final Form: December 4, 2007

In this contribution we propose a novel physical mechanism for microwave catalysis based on rotationally excited reactive species and verify its validity through a computer simulation of a realistic chemical reaction—neutral ester hydrolysis. This nonequilibrium system is formally described by introducing rotational temperature, which is higher than the translational temperature. A Born−Oppenheimer surface was constructed on the density functional theory level and applied to a modified Monte Carlo scheme. The simulation gave a reduced activation free energy when the rotational temperature was higher than the translational temperature, which constitutes a catalytic effect. For example, our calculation predicts that with rotational and translational temperatures of 310 and 300 K, respectively, the reaction should proceed 4.5 times faster than when both temperatures are 300 K. Moreover, this microwave catalytic effect is less pronounced at higher temperatures, which may have serious implications for the interaction of microwaves with living organisms in the context of widespread mobile telephony.

1. Introduction

In recent years, the use of microwaves has become a well-established technique in chemistry that has found numerous applications in the laboratory as well as in industry.[1−3] The main advantage of microwaves is to provide rapid heating, although other intriguing effects such as changed reaction selectivity and increased reaction rates have also been reported.[4−7] Despite the rapid spread of microwave use, understanding the mechanisms through which they influence chemical reactivity remains quite poor. The discussion of this matter has mainly been confined to an as yet unresolved debate over whether microwave catalysis is caused by thermal effects (such as local overheating) or some other "specific" (nonthermal) effects.[2,3] So far, this debate has been supported exclusively by experimental efforts whereas theoretical work on this topic remains surprisingly scarce.

Virtually all laboratory and industrial microwave sources operate at 2.45 GHz, corresponding to an oscillation time of 408 ps. This oscillation time is 2 orders of magnitude larger than the rotational correlation time for a single water molecule in bulk water (approximately 5 ps), meaning that isolated water molecules or small clusters of water molecules cannot efficiently absorb microwave energy. Only large clusters of water molecules have correlation times comparable to the oscillation time of microwaves and are therefore capable of direct absorption through the so-called dipolar polarization mechanism. This mechanism is believed to result mainly in librations, which are in part converted to molecular rotations. Accordingly, pure water absorbs microwaves relatively poorly. Absorption can be substantially improved by the addition of ionic species, which absorb microwave energy through the ionic conduction mechanism in which ions move with the oscillating electric field of microwaves. Their translatory motion is again, in part, converted to rotational motion of molecules in the vicinity of their movement path. Albeit with different efficiencies, both processes give rise to rotationally excited (hot) molecules.[3] During continuous microwave irradiation there is insufficient time for dissipation of the rotational energy into other degrees of freedom, which leads to a nonequilibrium situation. Formally, this situation can be described by a rotational temperature that is higher than the temperature governing other degrees of freedom. An analogous concept of spin temperatures that are different from the temperature of the environment is well established in the theory of NMR spectroscopy.[8]

In the sole quantum mechanical treatment of a rotationally excited diatomic molecule Miklavc demonstrated that it experiences altered statistics of collisions with other molecules (Figure 1).[9,10] An analogy can be made with the rotating blade of a lawnmower: as long as the translational motion (movement of the mower along the lawn) is much slower than the rotational motion of the blade all cutting of the grass is done by the blade tips. The entire blade will be cutting grass only in the case when rotation proceeds at velocities comparable or slower than translational motion will. Miklavc concluded that an analogously changed statistics of molecular collisions leads to a change in reaction kinetics.

The present study represents an extension of the approach developed by Miklavc, but rather than applying it to diatomic molecules, we used the principle of rotationally hot molecules resulting from microwave absorption in a realistic chemical reaction: neutral hydrolysis of the ester bond in methyl acetate. Cleavage of the ester bond is a reaction relevant in many biochemical as well as industrial processes.[11] In addition, we

* To whom correspondence should be addressed. E-mail: janez@kihp2.cmm.ki.si. Telephone: +386-1-4760200. Fax: +386-1-4760300.

† Abbrevations: PET, polyethylene terephthalate; MC, Monte Carlo; DFT, density functional theory; R, reactants; TS, transition state; T_r, rotational temperature; T_t, translational temperature; SCRF, solvent reaction field; EVB, empirical valence bond; MP2, Møller−Plesset perturbation of the second order.

10.1021/jp709766c CCC: $40.75

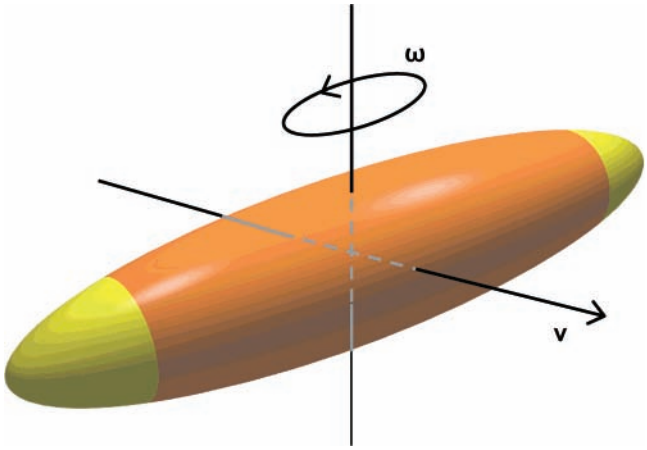

Figure 1. Schematic representation of a molecule with an anisotropic potential. The statistics of collisions with neighboring molecules depends on the translational (v) and angular (ω) velocities. In rotationally hot molecules the parts labeled in yellow represent areas of increased probability of molecular collisions giving rise to altered reactivity.

used it as a model for microwave assisted solvolysis of the ester bond in polyethylene terephthalate (PET) which was studied experimentally within our group.[12] We applied the concept of rotational excitation by first constructing the Born−Oppenheimer surface via quantum chemical methods, followed by a specifically developed Monte Carlo (MC) scheme that allowed the definition of different temperatures for translation and rotation. The purpose of this work was to demonstrate the catalytic power of rotationally hot species that result from microwave irradiation.

2. Computational Methods

Empirical Force Field. The studied chemical system consisted of one molecule of methyl acetate reacting with one water molecule.[13] Hydrolysis of the acetate gives rise to methanol and acetic acid, and the rate-limiting step for the reaction is the formation of a tetrahedral intermediate (Figure 2). The experimentally determined activation free energy for this rate-limiting step is 30 kcal/mol.[14,15] The activation free energy is defined as a free energy difference between the transition state and the reactants. Thus, to obtain the free energy barrier of the rate-limiting step of the studied reaction we only need to consider its reactants (ester and water) and the corresponding transition state, i.e., the saddle point (characterized by a single imaginary frequency) on the potential energy surface connecting the reactants and the unstable intermediate.

All calculations were performed at the B3LYP/3-21G level of theory encoded in the Gaussian03 suite of programs.[16] This density functional theory (DFT) method has the Becke three-parameter hybrid gradient corrected exchange functional[17] combined with the gradient-corrected correlation functional of Lee, Yang, and Parr.[18] We are aware of the significant empirical character of this method, but it does to some extent include the electron correlation. For the reactants a full geometry optimization was performed. The transition state structure was allocated using the Berny algorithm. The obtained geometries of the reactants and the transition state are depicted in Figure 3. The activation energy (a difference between energies of the transition state and the reactants) of 35.39 kcal/mol was calculated. Moreover, a vibrational analysis in the harmonic approximation was performed and only real frequencies for the reactants and a single imaginary frequency of 1354i cm^{-1} for the transition state were obtained. To check whether the correct transition structure was found, we performed a visualization of the vibration mode of this imaginary frequency using the MOLDEN program.[19] This mode should correspond to the reaction coordinate of the first step of the reaction mechanism presented in Figure 2. The vibration mode really coincided with the formation of a chemical bond between the carbonyl carbon of ester and the water oxygen, with the cleavage of the chemical bond connecting this water oxygen to the water hydrogen, and the formation of a chemical bond between this water hydrogen and the carbonyl oxygen of ester thus confirming the allocation of the correct transition state structure. A zero point energy correction of −2.25 kcal/mol was calculated for the free energy barrier. Finally, solvation effects were treated in the framework of the solvent reaction field (SCRF) method of Tomasi and coworkers.[20] A hydration free energy correction of −2.96 kcal/mol was found for the activation free energy. The solvent (water) accelerates the reaction because the transition state is better solvated than the reactants. When all three numbers were summed up, an activation free energy of 30.18 kcal/mol was obtained, in excellent agreement with the experimental value of 30 kcal/mol.[14,5] All in all, the B3LYP/3-21G level of theory (among several Hartree−Fock, DFT, and MP2 levels applied) most faithfully reproduces the energetics of the studied chemical reaction and is at the same time computationally affordable. Consequently, it was applied for the construction of the empirical force field.

To study the nonequilibrium state excited by microwaves and characterized by the three rotational degrees of freedom at a higher temperature than the three translational degrees of freedom, an empirical force field that separates rotations from translations had to be devised. The relative orientation of two rigid bodies is uniformly defined by three Eularian angles (ϕ, θ, ψ) and their relative position by three Cartesian coordinates (x, y, z).[21,22] Because almost no deformation of the water and methyl acetate molecules occurs upon transition from the reactants to the transition state (Figure 3), this methodology offers a suitable framework for the studied reaction. A simple parabolic potential energy function that enables the decomposition of the potential energy (V_{tot}) into translational (V_t) and rotational (V_r) contributions was used

$$V_{tot}^{Q} = V_{t}^{Q} + V_{r}^{Q} \quad (1)$$

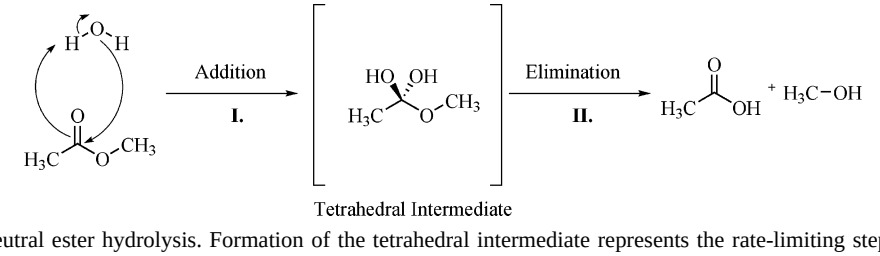

Figure 2. Scheme of neutral ester hydrolysis. Formation of the tetrahedral intermediate represents the rate-limiting step.

$$V_t^Q = \frac{1}{2}K_x^Q(x - x_0^Q)^2 + \frac{1}{2}K_y^Q(y - y_0^Q)^2 + \frac{1}{2}K_z^Q(z - z_0^Q)^2 \quad (2)$$

$$V_r^Q = \frac{1}{2}K_\phi^Q(\phi - \phi_0^Q)^2 + \frac{1}{2}K_\theta^Q(\theta - \theta_0^Q)^2 + \frac{1}{2}K_\psi^Q(\psi - \psi_0^Q)^2 \quad (3)$$

where Q represents either the reactant (R) or the transition state (TS) structure and harmonic force constants are denoted by K.

The reactant geometry served as a starting point for the parametrization. Zero values of the equilibrium Eulerian angles were assigned to the reactant orientation of the water molecule (ϕ_0^R, θ_0^R, ψ_0^R). The nonsingularity of Eulerian angles at zero θ value was avoided by the use of the *xyz convention* traditionally applied in U.S. and British aerodynamics studies.[23] The position of the water oxygen atom defined the equilibrium Cartesian coordinates for the reactant structure of the water molecule (x_0^R, y_0^R, z_0^R). Then, one of the six variables (for example ϕ) was changed from its equilibrium value and a corresponding new reactant geometry was obtained. This structure served as a starting point for the geometry optimization of the intramolecular internal coordinates at the B3LYP/3-21G level of theory, while the intermolecular internal coordinates were kept frozen. This procedure implies that vibrational degrees of freedom follow the rotational and translational motion giving rise to a relaxed force field. The continuous solvation model was not applied because it is inadequate for the description of nonequilibrium processes and nuclear quantum effects were neglected. In this way energies of three points with different ϕ values were collected, before the force constant K_ϕ^R was determined from the least-square fit method. The same procedure was applied for each of the remaining five variables.

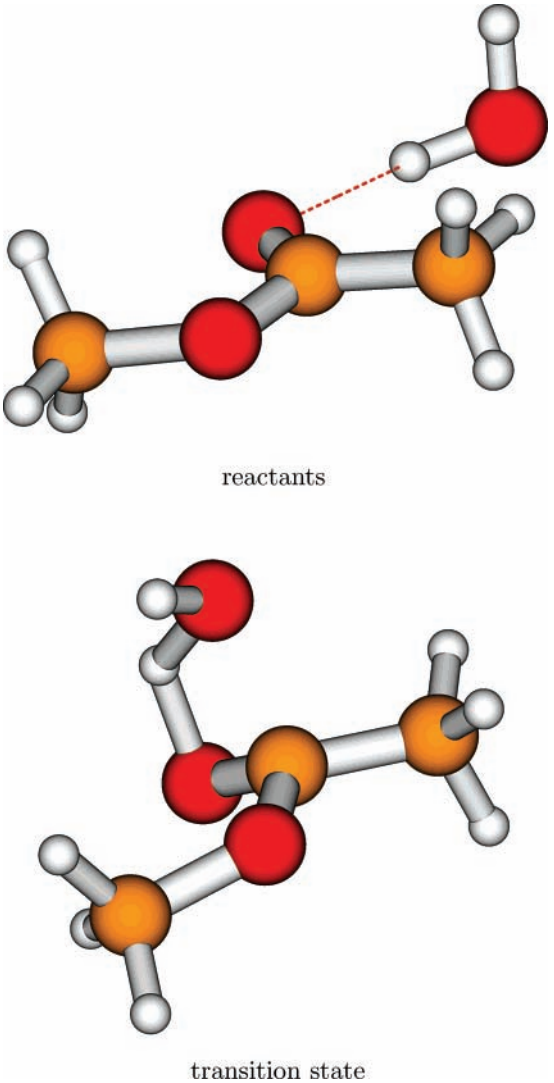

Figure 3. B3LYP/3-21G calculated geometries of the reactants and the transition state. Oxygen is depicted in red, carbon in orange, and hydrogen in white.

TABLE 1: Force Field Parameters[a]

	R	TS		R	TS
K_x [kcal mol^{-1} Å^{-2}]	51.6	75.0	x_0 [Å]	3.006	−0.116
K_y [kcal mol^{-1} Å^{-2}]	5.50	296.	y_0 [Å]	0.012	−1.632
K_z [kcal mol^{-1} Å^{-2}]	28.8	96.0	z_0 [Å]	0.325	1.947
K_ϕ [kcal mol^{-1} rad^{-2}]	8.64	57.6	ϕ_0 [rad]	0.	1.857
K_θ [kcal mol^{-1} rad^{-2}]	24.4	94.8	θ_0 [rad]	0.	0.825
K_ψ [kcal mol^{-1} rad^{-2}]	20.6	88.0	ψ_0 [rad]	0.	−0.135

[a] Harmonic force constants, equilibrium Cartesian coordinates, and equilibrium Eulerian angles of the empirical force field for reactants (R) and the transition state (TS).

The transition state is an elevated part of the phase-space dividing reactants and products, which is formally represented by an ensemble of structures corresponding to a given temperature.[24] To obtain such an ensemble, an inverted potential energy surface must be constructed where the transition state structure is allocated by minimization.[25,26] The position (described by the following equilibrium parameters: x_0^{TS}, y_0^{TS}, z_0^{TS}) of the water molecule in the transition state geometry was defined by the Cartesian coordinates of its oxygen atom in the coordinate system of the reactants. The orientation of the water molecule for the transition state structure in the coordinate system of the reactants (defined by the following equilibrium parameters: ϕ_0^{TS}, θ_0^{TS}, ψ_0^{TS}) was determined by the least-squares fit method. Force constants were obtained using the same procedure as for the reactants. All together $2 \times 6 \times 3 = 36$ constrained geometry optimizations were performed. The reaction coordinate corresponds to the y-axis (direction perpendicular to the plane of the carbonyl group), as demonstrated by the negative K_y^{TS} force constant. Its value had to be inverted to allow for thermal averaging in the transition state region.[27]

All empirical parameters applied in the potential energy function for the reactants and the transition state are presented in Table 1. It should be noted that the Eulerian angle force constants corresponding to the transition state are significantly larger than those corresponding to the reactants. This can be understood in view of the more rigid (product-like) nature of the transition state structure. The constructed empirical force field has a computationally inexpensive form that allows for subsequent Monte Carlo simulation. We did not set up the empirical valence bond (EVB) reactive surface, because it does not facilitate a simple separation of rotational and translational degrees of freedom.

Monte Carlo Simulation. A novel Monte Carlo method that simultaneously generates ensembles of structures on the reactant potential energy surface as well as on the inverted potential energy surface of the transition state was devised. The Metropolis scheme was adapted to operate at two different temperatures. The lower temperature governed the translations (T_t) and the higher temperature corresponded to the microwave excited rotations (T_r). The MC simulation scheme presented in Figure 4 was started by choosing simultaneously nonminimum water geometries for the reactants (x_1, y_1, z_1, ϕ_1, θ_1, ψ_1) with corresponding translational ($V_{1,t}^R$) and rotational ($V_{1,r}^R$) potential energy and for the transition state ($x_{1'}$, $y_{1'}$, $z_{1'}$, $\phi_{1'}$, $\theta_{1'}$, $\psi_{1'}$) with corresponding translational ($V_{1',t}^{TS}$) and rotational ($V_{1',r}^{TS}$) poten-

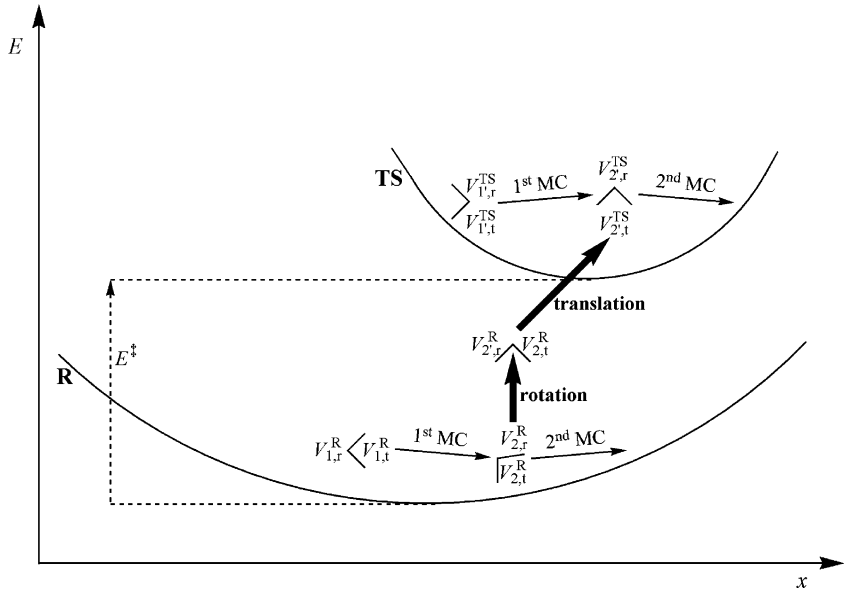

Figure 4. Scheme of Monte Carlo simulation. The jump from the reactant well (R) to the transition state region (TS) is composed of a rotation in the R region, followed by translation to the TS structure. For details and definition of symbols see Computational Methods.

tial energy (transition state geometries are labeled with primes). Trial reactant and transition state structures were then obtained by creating small random displacements in each of the three Cartesian coordinates and in the two Eulerian angles. To fulfill the condition of microscopic reversibility small random displacements in cos θ rather than in θ were chosen. [22] The size of the maximum displacements was set to keep the acceptance rate of about 50%. The generated reactant geometry (x_2, y_2, z_2, ϕ_2, θ_2, ψ_2) with corresponding translational ($V^{R}_{2,t}$) and rotational ($V^{R}_{2,r}$) potential energy was accepted with the probability of

$$P^{R} = \min\left\{\exp\left(-\frac{V^{R}_{2,t} - V^{R}_{1,t}}{k_B T_t}\right)\exp\left(-\frac{V^{R}_{2,r} - V^{R}_{1,r}}{k_B T_r}\right),1\right\} \quad (4)$$

where k_B represents the Boltzmann constant. The generated transition state structure ($x_{2'}$, $y_{2'}$, $z_{2'}$, $\phi_{2'}$, $\theta_{2'}$, $\psi_{2'}$) with corresponding translational ($V^{TS}_{2',t}$) and rotational ($V^{TS}_{2',r}$) potential energy was accepted with the probability of

$$P^{TS} = \min\left\{\exp\left(-\frac{V^{TS}_{2',t} - V^{TS}_{1',t}}{k_B T_t}\right)\exp\left(-\frac{V^{TS}_{2',r} - V^{TS}_{1',r}}{k_B T_r}\right),1\right\} \quad (5)$$

We were interested in obtaining the probability of a jump from the reactant to the transition state structure ($P^{R\rightarrow TS}$). The total potential energy required for this transition is

$$V^{R\rightarrow TS}_{tot} = E^{\ddagger} - V^{R}_{2,tot} + V^{TS}_{2',tot} - K^{TS}_{y}(y_{2'} - y^{TS}_{0})^2 \quad (6)$$

where $E^{\ddagger}$ represents the activation energy of 35.39 kcal/mol obtained from calculations at the B3LYP/3-21G level of theory. Simulation that spans over such large energy differences would normally require biased sampling. However, in contrast to conventional simulations of reactive systems we knew the exact transition state geometries. Because the transition state was simulated as a minimum on a potential energy surface inverted along the *y*-axis (the reaction coordinate), the last term of eq 6 was used to eliminate the effect of this inversion. To decompose the total potential energy of the jump into rotational and translational contributions, a simplification that all rotation takes place on the reactant potential energy surface was made. This assumption can be corroborated by the fact that the reaction coordinate coincides with the *y*-axis, so in the vicinity of the transition state mainly translation is taking place. The stronger angular dependence of the potential energy indicated by larger angular force constants of the transition state structure in comparison with the reactants confirms this simplification as well. Our computational approach where we assume that the reactivity is controlled by the reactant orientation is also justified by the fact that excited rotations proceed faster than translations and have, therefore, enough time to adjust to any translational change imposed upon the reacting system.[28] Rotation in the reactant well leads to an intermediate geometry (x_2, y_2, z_2, $\phi_{2'}$, $\theta_{2'}$, $\psi_{2'}$) with corresponding translational ($V^{R}_{2,t}$) and rotational ($V^{R}_{2',r}$) potential energy. The rotational portion of the potential energy required for the jump from the reactants to the transition state is therefore given by

$$V^{R\rightarrow TS}_{r} = V^{R}_{2',r} - V^{R}_{2,r} \quad (7)$$

Because the transitional portion can be obtained by subtracting the rotational portion from the total potential energy, the probability of this jump can be written as

$$P^{R\rightarrow TS} = \exp\left(-\frac{V^{R\rightarrow TS}_{tot} - V^{R\rightarrow TS}_{r}}{k_B T_t}\right)\exp\left(-\frac{V^{R\rightarrow TS}_{r}}{k_B T_r}\right) \quad (8)$$

New trial reactant and transition state structures were then generated and the whole procedure was repeated for 10^8 times when convergence in average value of the probability $P^{R\rightarrow TS}$ was attained.

A series of the described Monte Carlo simulations was performed for different rotational temperatures at a fixed translational temperature of 300 K. The average probabilities for a jump from the reactant to the transition state structure were converted into activation free energies ($G^{\ddagger}$) via the relation[29]

$$G^{\ddagger} = -k_B T \ln\langle P^{R\rightarrow TS}\rangle \quad (9)$$

where angular brackets denote averaging and *T* stands for the equilibrium thermodynamic temperature, which is equal to the

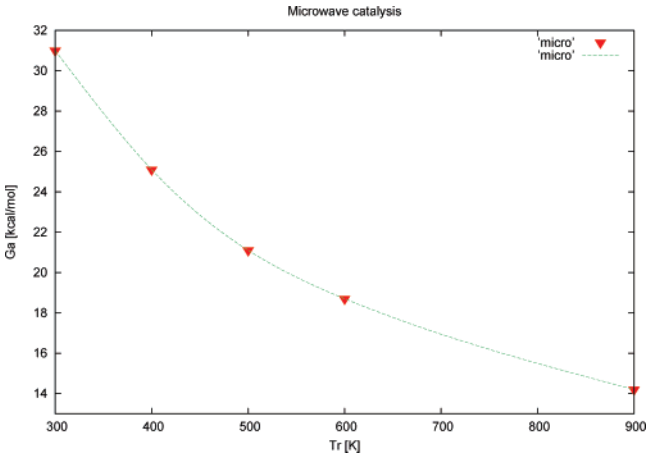

Figure 5. Free energy of activation (G_a) as a function of rotational temperature (T_r). Translational temperature was set to 300 K.

translational temperature of 300 K. In the absence of microwave irradiation, an equilibrium state with equal translational and rotational temperature of 300 K is maintained. Under such conditions the reaction barrier of 31.0 kcal/mol was obtained, which is in very good agreement with the experimental value of 30 kcal/mol.[14,15] The uncertainty of this result (0.2 kcal/mol) was calculated as the standard deviation of independent simulations applying different random seed values.

3. Results and Discussion

The catalytic effect at a given rotational temperature is the activation free energy difference relative to the situation in which $T_r = T_t$. In this we followed the approach of Warshel to enzymatic catalysis, where the catalytic effect for an enzymatic reaction is calculated relative to the corresponding reference reaction without the enzyme.[30,31] In our case the elevated T_r is the catalyst. Clearly the different rotational temperatures correspond to different distribution widths of the probability densities. In the case of a higher rotational temperature the population of the reactant states that correspond to the minimum of the TS surface is higher, giving rise to enhanced probability of the reactive event.

Figure 5 shows the dependence of activation free energy for the reaction on rotational temperature, while the translational temperature is held constant at 300 K. It clearly indicates that the free energy barrier is reduced with hotter rotations. The reduction is most pronounced at smaller differences between T_r and T_t. As the difference between the temperatures increases this reduction becomes less intense. Results show that at $T_r =$ 310 K and $T_t = 300$ K the activation free energy is lowered by 0.9 kcal/mol. Assuming the validity of the transition state theory this difference would cause the reaction to proceed 4.5 times faster than without microwave irradiation ($T_r = T_t = 300$ K).

We compared our results with experimental results obtained from polyethylene terephthalate (PET) depolymerization with and without the use of microwaves.[12] The experiments performed at 573 K gave an approximately 18-fold increase in reaction rate when microwaves were used as the sole energy source. Using our truncated system, we were able to reproduce the experimental acceleration by setting the rotational temperature 90 K higher than the translational temperature (573 K). It is interesting that the same reaction rate increase could be obtained with a rotational temperature only 20 K higher vs a translational temperature of 300 K. The fact that the microwave effect is more pronounced at lower temperatures is particularly interesting in the context of microwave interaction with living organisms, which has been subject of much speculation in relation to mobile telephony and radars. If microwaves were to catalyze biochemical reactions taking place in living organisms, it is easy to envision pathological effects. For example, enhancing the reaction between ultimate carcinogens and DNA could contribute to the occurrence of tumors.[32,33] Despite much speculation, epidemiological evidence of such effects remains scarce.[34,35] An intriguing suggestion of microwave effects is offered by a study on nematodes, which produced heat stress proteins when exposed to microwaves, although no temperature rise could be measured.[36]

At this point, a reference should be made to the most widely accepted explanation of "the microwave effect", which is believed to be purely thermal and to occur through local hotspots that cannot be adequately measured. As expected, the higher temperature at these spots significantly accelerates reactions. However, in the case of competing reactions with different activation energies selectivity should in fact decrease with higher temperature. This is in disagreement with the numerous experimental results where the use of microwaves enhances chemo-, regio-, and stereoselectivity.[6,7] On the other hand, the altered molecular collision statistics proposed in this Letter can lead to higher reaction selectivity due to the different shapes of the Born−Oppenheimer surfaces for the competing reactions.

4. Conclusions

This work offers a novel proposal for the physical mechanism of microwave catalysis based on rotationally excited states. The approach was verified through a computer simulation of microwave catalysis in a realistic chemical reaction in which an elevated rotational temperature was introduced as an ad hoc parameter. The introduction of elevated rotational temperature in the simulation resulted in lowering the activation free energy and in a corresponding increase of the reaction rate. Finally, it should be said that the system and the simulation protocol leave plenty of space for improvement. It remains a challenge to perform nonequilibrium molecular dynamics simulation of a reactive species, the solvent, and ions in an external electromagnetic field. This would require the development of novel simulation protocols as well as huge amounts of computer power, making better understanding of microwave catalysis a goal for the future. On the experimental field it would be interesting to see if raising the microwave frequency would decrease dissipation of rotational energy resulting in an enhanced microwave catalytic effect.

Acknowledgment. This Letter is dedicated to the memory of Professor Adolf Miklavc. Financial support from the Slovenian Ministry of Science and Education through grant P1-0012 is gratefully acknowledged.

References and Notes

(1) Larhed, M.; Moberg, C.; Hallberg, A. *Acc. Chem. Res.* **2002**, *35*, 717.
(2) Kingston, H. M.; Haswell, J. S. *Microwave-Enhanced Chemistry*; American Chemical Society: Washington, DC, 1997.
(3) Kappe, C. O.; Stadler, A. *Microwaves in Organic and Medicinal Chemistry*; Wiley: Weinheim, 2005.
(4) Bohr, H.; Bohr, J. *Phys. Rev. E* **2000**, *61*, 4310.
(5) Blanco, C.; Auerbach, S. M. *J. Am. Chem. Soc.* **2002**, *124*, 6250.
(6) Favretto, L.; Nugent, W. A.; Licini, G. *Tetrahedron Lett.* **2002**, *43*, 2581.
(7) de la Hoz, A.; Diaz-Ortiz, A.; Moreno, A. *Curr. Org. Chem.* **2004**, *8*, 903.
(8) Ernst, R. R.; Bodenhausen, G.; Wokaun, A. *Principles of Nuclear Magnetic Resonance in One and Two Dimensions*; Clarendon Press: Oxford, U.K., 1991.

(9) Miklavc, A. *Chem. Phys. Chem.* **2001**, *2*, 552.
(10) Miklavc, A. *J. Chem. Phys.* **2004**, *121*, 1171.
(11) Lensink, M. F.; Mavri, J.; Berendsen, H. J. C. *J. Comput. Chem.* **1999**, *20*, 886.
(12) Kržan, A. *Polym. Adv. Technol.* **1999**, *10*, 603.
(13) Wolfe, S.; Kim, C.-K.; Yang, K.; Weinberg, N.; Shi, Z. *J. Am. Chem. Soc.* **1995**, *117*, 4240.
(14) Gillan, C. J.; Knipe, A. C.; Watts, W. E. *Tetrahedron Lett.* **1981**, *22*, 597.
(15) Isaacs, N. S. *Physical Organic Chemistry*; Longman Scientific & Technical: England, 1987.
(16) Frisch, M. J.; Trucks, G. W.; Schlegel, H. B.; Scuseria, G. E.; Robb, M. A.; Cheeseman, J. R.; Montgomery, J. A.; Vreven, T.; Kudin, K. N.; Burant, J. C.; Millam, J. M.; Iyengar, S. S.; Tomasi, J.; Barone, V.; Mennucci, B.; Cossi, M.; Scalmani, G.; Rega, N.; Petersson, G. A.; Nakatsuji, H.; Hada, M.; Ehara, M.; Toyota, K.; Fukuda, R.; Hasegawa, J.; Ishida, M.; Nakajima, T.; Honda, Y.; Kitao, O.; Nakai, H.; Klene, M.; Li, X.; Knox, J. E.; Hratchian, H. P.; Cross, J. B.; Adamo, C.; Jaramillo, J.; Gomperts, R.; Stratmann, R. E.; Yazyev, O.; Austin, A. J.; Cammi, R.; Pomelli, C.; Ochterski, J. W.; Ayala, P. Y.; Morokuma, K.; Voth, G. A.; Salvador, P.; Dannenberg, J. J.; Zakrzewski, V. G.; Dapprich, S.; Daniels, A. D.; Strain, M. C.; Farkas, O.; Malick, D. K.; Rabuck, A. D.; Raghavachari, K.; Foresman, J. B.; Ortiz, J. V.; Cui, Q.; Baboul, A. G.; Clifford, S.; Cioslowski, J.; Stefanov, B. B.; Liu, G.; Liashenko, A.; Piskorz, P.; Komaromi, I.; Martin, R. L.; Fox, D. J.; Keith, T.; Al-Lahram, M. A.; Peng, C. Y.; Nanayakkara, A.; Challachombe, M.; Gill, P. M. W.; Johnson, B.; Chen, W.; Wong, M. W.; Gonzales, C.; Pople, J. A. *Gaussian 03*, revision B.03; Gaussian, Inc.: Wallingford, CT, 2004.
(17) Becke, A. D. *J. Chem. Phys.* **1993**, *98*, 5648.
(18) Lee, C.; Yang, W.; Parr, R. G. *Phys. Rev. B* **1998**, *37*, 785.
(19) Schaftenaar, G.; Noordik, J. H. *J. Comput.-Aided Mol. Des.* **2000**, *14*, 123.
(20) Miertus, S.; Scrocco, E.; Tomasi, J. *Chem. Phys.* **1981**, *55*, 117.
(21) Frenkel, D.; Smit, B. *Understanding Molecular Simulation*; Academic Press: San Diego, 1996.
(22) Allen, M. P.; Tildesley, D. J. *Computer Simulation of Liquids*; Claderon Press: Oxford, U.K., 1989.
(23) Goldstein, H. *Classical Mechanics*; Addison-Wesley: London, 1980.
(24) Jensen, F.; Norrby, P.-O. *Theor. Chem. Acc.* **2003**, *109*, 1.
(25) Norrby, P.-O.; Rasmussen, T.; Haller, J.; Strassner, T.; Houk, K. N. *J. Am. Chem. Soc.* **1999**, *121*, 10186.
(26) Eksterowicz, J. E.; Houk, K. N. *Chem. Rev.* **1993**, *93*, 2439.
(27) Norrby, P.-O. *J. Mol. Struct. (THEOCHEM)* **2000**, *506*, 9.
(28) Miklavc, A.; Perdih, M.; Smith, I. W. *J. Chem. Phys.* **2000**, *112*, 8813.
(29) Leach, A. R. *Molecular Modeling*; Prentice Hall: Harlow, 2001.
(30) Warshel, A. *Computer Modeling of Chemical Reactions in Enzymes and Solutions*; Wiley: New York, 1991.
(31) Warshel, A.; Florian, J. *Proc. Natl. Acad. Sci. U.S.A.* **1998**, *95*, 5950.
(32) Bren, U.; Guengerich, F. P.; Mavri, J. *Chem. Res. Toxicol.* **2007**, *20*, 1134.
(33) Kranjc, A.; Mavri, J. *J. Phys. Chem. A* **2006**, *110*, 5740.
(34) Parascandola, M. *Science* **2001**, *294*, 1440.
(35) Hardell, L.; Carlberg, M.; Söderqvist, F.; Mild, K. H.; Morgan, L. L. *Occup. Environ. Med.* **2007**, *64*, 626.
(36) de Pomerai, D.; Daniells, C.; David, H.; Allan, J.; Duce, I.; Mutwakil, M.; Thomas, D.; Sewell, P.; Tattersall, J.; Jones, D.; Candido, P. *Nature* **2000**, *405*, 417.